JOURNAL OF MATERIALS SCIENCE 13 (1978) 341–350

Hot-pressing and the α-β phase transformation in silicon nitride

L. J. BOWEN, R. J. WESTON, T. G. CARRUTHERS, R. J. BROOK
Department of Ceramics, University of Leeds, UK

The kinetics of densification and the kinetics of the α–β phase transformation have been measured during the hot-pressing of silicon nitride ceramics using magnesia as additive. Two mechanisms of densification have been identified. The first is a very rapid particle rearrangement, liquid-enhanced above 1550° C, which operates up to relative densities of about 0.65. The kinetics of the much slower decelerating second stage obey the Coble hot-pressing equation and the rate of densification is found to be proportional to the amount of additive. The controlling mechanism is believed to be diffusion in a boundary second phase, and values for the diffusion coefficient, D_b, of the rate-controlling species in the boundary phase for temperatures above and below 1550° C are given. The kinetics of the α to β transformation, the greater part of which occurs after densification is complete, are described by a first order reaction; the dependence of rate on the quantity of additive and on temperature is similar to that found for densification, and a similar controlling mechanism is believed to be responsible for the two processes.

1. Introduction

Silicon nitride is widely recognised as a material with much potential for high temperature engineering applications. Ceramic specimens have in general been prepared by two alternative routes giving rise to two types of material, reaction bonded silicon nitride and hot-pressed silicon nitride.

The reaction bonding process is complex and incompletely understood although models for the reaction sequence are now available for well defined conditions [1]. The hot-press process, which requires the use of additives (e.g. MgO, Y_2O_3), has been studied in terms of microstructural observations [2]; phase analysis of the grain boundary material [3, 4], and kinetics of densification [5]. Ambiguities of interpretation have been recognised, particularly in the treatment of kinetic data [5], and a firm model for the process has yet to be proposed.

Silicon nitride exists in two structural forms, known as α and β [6]; it is well known [7] that α silicon nitride can be hot-pressed more readily than the β form and that transformation from α to β occurs during hot-pressing, mainly after the completion of densification [8, 5]. Apart from microstructural work [2], little attention has been paid to the mechanism of the conversion and its effect upon the properties of the resulting hot-pressed silicon nitride.

The objective of the present paper is to describe complementary studies of the kinetics of hot pressing and of the kinetics of the α–β phase transformation during and after hot pressing, using high purity (99.9%) α silicon nitride with magnesia as additive; it will be seen that similar features occur in the two sets of kinetics suggestive of a common mechanism for the two processes.

2. Experimental

2.1. Materials

The silicon nitride powder used for all the kinetic experiments was closely similar to that used by one of the present authors in an earlier study [8] and was made by the Allen Clark Research Laboratories of the Plessey Co. Ltd., from silicon powder of 99.9% purity. Spectrographic analysis by the makers showed the following levels of impurity: Fe < 0.1%, Cu < 0.01%, Al < 0.01%, Ca < 0.001%, Na and K not detected. The α silicon nitride con-

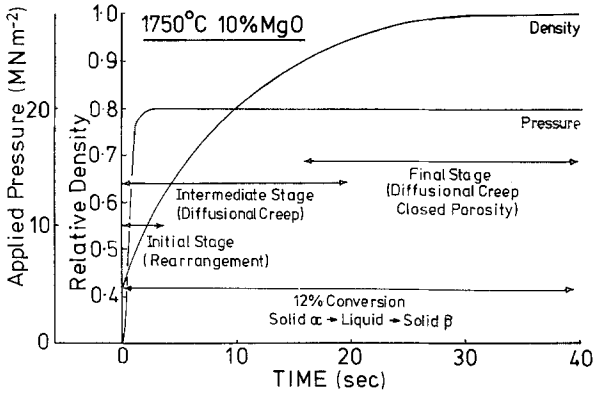

Figure 1 Diagrammatic summary of the processes occurring during densification. Based on data for high α silicon nitride powder containing 10% MgO hot-pressed at 1750° C under a pressure of 20 MN m^{-2}.

tent was shown by X-ray diffractometry and microdensitometry to be 95 ± 5%. The surface area, measured by BET nitrogen adsorption, was 12.5 m^2 g^{-1} giving an equivalent mean spherical diameter of 0.15 μm. Transmission electron microscopy showed the powder to be made up of aggregates of equiaxed grains interspersed with some lath-like particles which were occasionally up to 10 μm in length, but the overall picture was not inconsistent with the mean crystallite size previously given.

All other chemicals used were of "AnalaR" grade. Additives were mixed with the silicon nitride powder by mechanical stirring as an aqueous slurry and subsequent drying.

2.2 Hot-pressing procedures

The hot-pressing apparatus and its associated control and monitoring equipment have been described in detail previously [8]. Nuclear grade graphite dies and high-density graphite punches, coated on the contact surfaces with a thin wash of high purity boron nitride powder, were used to produce compacts 25 mm in diameter weighing about 12 g. The required hot-pressing pressure was applied to the cold compact and released; the die was then heated at about 100° C min^{-1} and the pressure reapplied within a period of 2 to 3 sec, immediately the chosen hot-pressing temperature was reached. Temperature could be held constant to better than ±5° C for long periods and pressure maintained constant to ±2% by means of a gas ballast hydraulic accumulator. When power was cut off at the end of the hot-pressing cycle, initial cooling was rapid enough to prevent any significant changes occurring in the compacts during cooling. In assessing the density achieved during hot-pressing, a theoretical density of 3200 kg m^{-3} was assumed for silicon nitride containing 5 wt % MgO.

2.3. Phase analysis

The α and β phase content of samples that had been hot-pressed for different times, temperatures, and pressures was determined. Crystallographic analysis was undertaken by X-ray diffractometry at a scanning speed of $\frac{1}{2}°2\theta$ min^{-1} using Cu$K\alpha$ radiation on samples crushed to pass a 350 mesh (50 μm) sieve. α:β ratios were determined from the ratio of the peak heights of the α_{102} and β_{210} reflections, and the α content could be assessed to better than ±3%.

3. Results

3.1. Densification kinetics

Initial experiments confirmed that, in the absence of an additive, the α silicon nitride powder could not be densified to any significant extent by hot-pressing below 1750° C; above this temperature slight densification was accompanied by increasingly severe decomposition. The addition of 5 wt % MgO enabled near theoretical density to be attained at all temperatures over about 1450° C at rates which were markedly temperature- and pressure-dependent. Under comparable conditions the fine-grained high α silicon nitride powder used in this work densified at much greater rates than the powders used by other workers [5]; very rapid densification occurred immediately pressure was applied, followed by a period of slower densification. It is convenient to treat these stages separately although, as seen in Fig. 1, a degree of overlap is to be expected.

3.2. First stage: particle re-arrangement

When pressure was applied above 1550° C to compacts containing greater than 5 wt % MgO, the relative density increased to about 0.6 within the period of 3 sec needed to establish the desired pressure; this made it difficult to obtain useful

kinetic data for this stage of the process. Wild *et al.* [9] have postulated that a magnesium silicate liquid exists within the compact above 1550° C which makes possible a tapid liquid-enhanced particle re-arrangement process. This brings about dense random packing of the crystallites together with partial filling of the voids by liquid. However, at these temperatures it is not possible to exclude other contributions to densification arising from particle deformation processes such as plastic deformation (particularly under the high local stresses encountered at points of contact) or solution–precipitation. Using MgO as an additive, it is difficult to distinguish between the effects of such simultaneous processes.

If lithia is used in place of MgO, a lithium silicate liquid should be formed at about 1200° C. At such a temperature, the occurrence of plastic flow or solution precipitation processes should be less marked and the operation of the liquid enhanced particle re-arrangement process should therefore be more readily distinguished. Accordingly, hot-pressings of the silicon nitride with 5 wt% Li_2O were made at 1200 and 1300° C and, although at both temperatures a relative density of about 0.65 was attained within a few seconds, no further densification was detectable even after prolonged periods of hot-pressing. Particle deformation was observed on raising the temperature, when densification was seen to occur at temperatures above 1450° C, the rate increasing rapidly with rising temperature.

Additional evidence that the early stage of densification is liquid-enhanced was obtained by heating silicon nitride powder containing 5 wt% MgO in the hot-pressing die to 1600° C without pressure and cooling it to 1300° C. If pressure was then applied, fairly rapid densification to a relative density of 0.5 occurred. It is believed that this preheating treatment allowed a magnesium silicate liquid to form and be retained as a viscous glass which subsequently allowed rearrangement to take place.

The absence of any significant α–β transformation during the initial rapid densification process, even at temperatures well in excess of 1550° C, points to an alternative source of silica to that suggested by Wild *et al.* [9], who have proposed that some of the silica required to form the liquid is rejected from the α nitride lattice during transformation to the β form. One possibility for the alternative source, is the coating of oxide known to cover the nitride particles. If a surface area of 12.5 $m^2 g^{-1}$ is assumed for the crystallites, calculation shows that a surface layer of amorphous silica 2.5 nm thick is sufficient to convert 5 wt% MgO to about 12 vol% liquid of eutectic composition.

These experiments provide clear evidence that the observed immediate rapid densification is brought about by the formation of a liquid phase (possibly assisted by a small amount of particle deformation above about 1450° C), and that particle rearrangement ceases to be effective as a densification process at a relative density corresponding to that of close random packing with some filling of pores by liquid. At the level of additive used the maximum density attainable is about 0.65 to 0.70; further densification requires a process involving change in shape of the particles.

3.3. Second stage: particle deformation

Change in crystallite shape is involved during the whole of the subsequent deformation covering densities from about 0.65 to 1.0. During the final stage, the elimination of entrapped gases from sealed pores is also necessary; under hot-pressing conditions, however, the amount of residual porosity is very small at the point where the pressure of entrapped gases prevents further densification, and no attempt will be made in the following to consider the final stage separately.

Fig. 2 shows the effect of variations in temperature at constant pressure on the densification rate of silicon nitride containing 5 wt% MgO. The curves shown represent typical examples of the smoothed average curves obtained from at least ten separate hot-pressings under each condition. They were found to be extremely reproducible with little variation in shape or absolute position from run to run.

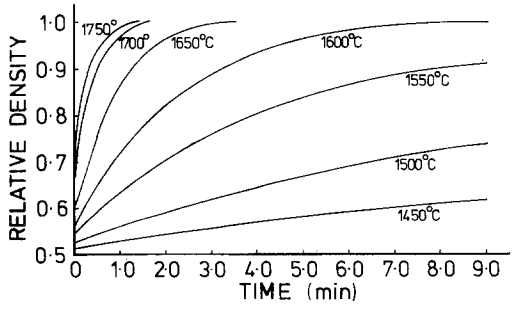

Figure 2 Dependence of densification rate of silicon nitride, containing 5% MgO, on temperature at a constant applied pressure of 20 MN m^{-2}.

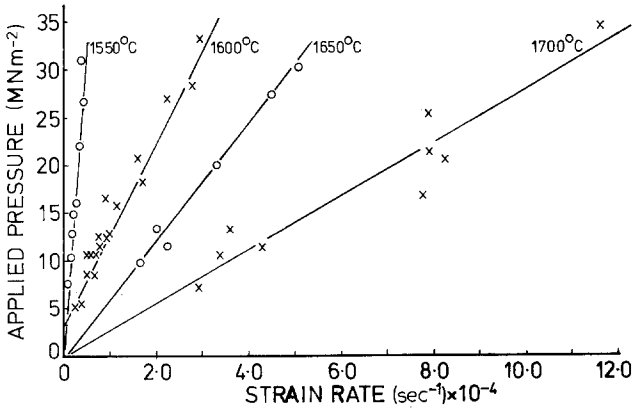

Figure 3 Linear dependence of strain rate, at a constant relative density of 0.75, on applied pressure for silicon nitride containing 5% MgO.

The interpretation of such data can be most usefully attempted in terms of the atomic processes capable of producing densification, and of the rate-controlling steps in these processes. Once the particle re-arrangement stage is completed, five possible mechanisms of further densification merit consideration: (i) plastic flow in the crystallites by dislocation movement; (ii) viscous flow of a vitreous grain boundary phase; (iii) deformation of the grains by lattice diffusion (Nabarro–Herring creep [10]); (iv) deformation by grain boundary diffusion (Coble creep [11]); (v) liquid-phase solution–precipitation sintering (Kingery [12]).

The first of these may be eliminated as a mechanism responsible for the densification of α silicon nitride with MgO because of the very nearly linear dependence of the strain rate $\dot{\epsilon} = -\frac{1}{\rho}\frac{d\rho}{dt}$ at constant density on the applied pressure as shown in Fig. 3. This is distinct from the power law dependence, $\dot{\epsilon} = k\sigma^n$ (σ = applied stress) encountered when dislocation mechanisms are operative where n has values typically greater than 2 [13]. The absence of dislocation networks on transmission electron micrographs of the fully dense hot-pressed α silicon nitride examined during the present work, also supports the rejection of this mechanism.

The second mechanism is also an unsatisfactory explanation for densification in that it cannot produce the reshaping of the solid grains which, with the available amount of liquid phase, is necessary to fill the pore space remaining after particle re-arrangement is complete. As will be seen there is another reason for rejecting this mechanism.

Consequently, interpretation of the data becomes a matter of distinguishing between the last three processes. This can be attempted [5] for the hot-pressing of silicon nitride with MgO by comparing kinetic data with the derived expressions for creep (mechanisms (iii) and (iv)) using [14] the Murray equation [15] for densification of a continuous viscous medium:

$$\Delta \ln (1-\rho) = -K_c t \qquad (1)$$

and for liquid phase sintering (mechanism (v)) using the Kingery equation [12]:

$$\Delta \ln \rho = K_e t^{1/n} \qquad (2)$$

where ρ is the relative density, t is time, K_c and K_e are constants, and $n = 3$ or 5 depending on the nature of the rate controlling process (solution into or diffusion through the liquid phase respectively). The equal success of both these expressions in fitting the data (Figs. 4 and 5) does not allow a firm choice between the two mechanisms. This ambiguity has been encountered in other hot-pressing studies [5].

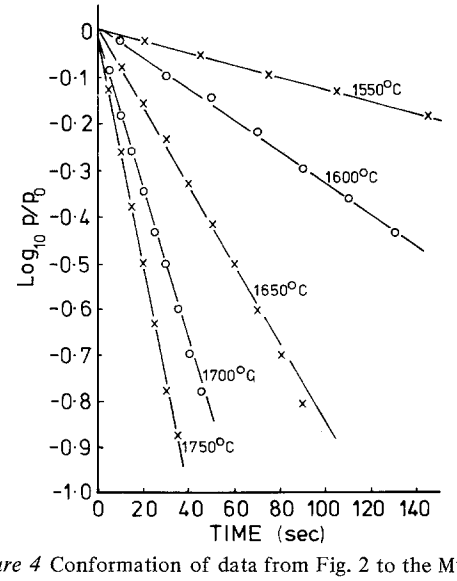

Figure 4 Conformation of data from Fig. 2 to the Murray [15] equation.

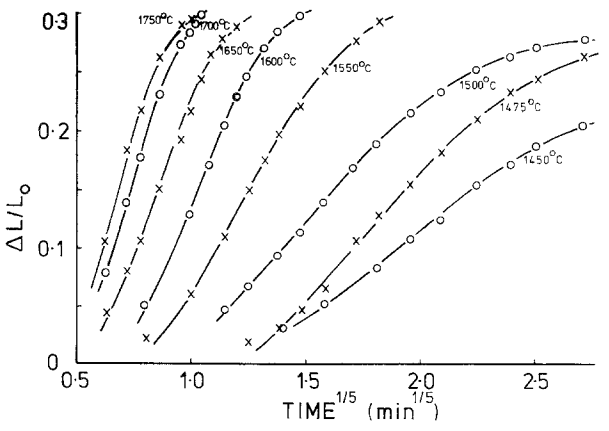

Figure 5 Conformation of data from Fig. 2 to the Kingery [12] equation.

An alternative approach is to analyse the data in terms of the Coble intermediate stage hot-pressing model [16], since this is equally applicable to creep by grain-boundary diffusion or to sintering by liquid phase processes [17]. Distinction between the two processes must then be made by making controlled changes in the experimental variables featuring in the Coble equation and explaining the resulting behaviour in terms of the structural models associated with the two processes.

The equation is used in the form [17]

$$\frac{d\rho}{dt} = \frac{47.5PD_b a^3 W}{G^3 kT} \qquad (3)$$

where P is the applied pressure, D_b the boundary diffusion coefficient and a^3 the volume of material transported for each atom of the rate controlling species; W is the boundary thickness and G the grain size. It is assumed that if the analysis is made at an early stage in the densification process, the surface energy term in the full equation [16] may be neglected. A test of this assumption may be made by taking the pore radius as equal to the grain size, and a value of $0.25\,J\,m^{-2}$ for the surface energy of the MgO/SiO_2 phase; the surface energy contribution is then $1.6\,MN\,m^{-2}$ in comparison with the applied loads, which range from 7 to $30\,MN\,m^{-2}$.

The applicability of the model, and further justification for omitting the surface energy term, are shown in Fig. 3. The densification rate at constant density is seen to vary linearly with applied pressure for a range of temperature and the negligible strain rate at zero stress indicates that the omission of the surface energy term is justified.

The equation is written in terms of densification rate at a given point in time rather than in terms of density achieved at a given point in time. This feature, which makes the model less sensitive to details of the geometry of the particle–particle contact, means that data are analysed by taking the densification rate at a given density (in the following, $\rho = 0.70$) for insertion in the left hand side of the equation.

It is shown that the specimens contain a second phase at the grain boundary; consequently, a first suggestion is that Equation 3 is applicable in its guise as a liquid-phase sintering equation [17]. In

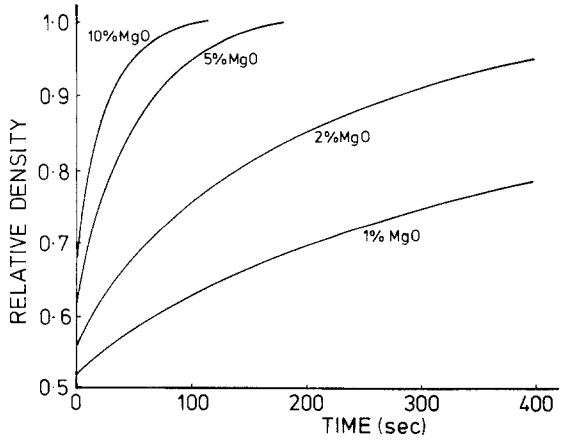

Figure 6 Densification curves for silicon nitride with varying MgO content pressed at 1650° C at a pressure of $20\,MN\,m^{-2}$.

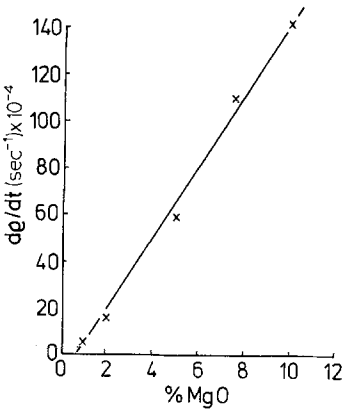

Figure 7 Instantaneous densification rates derived from Fig. 6 at a relative density of 0.7 as a function of MgO content.

this context, the terms W becomes the thickness of the boundary liquid-phase film; since W is then proportional to the total amount of liquid present, this suggests that the densification rate should be linearly dependent on the amount of MgO added. Fig. 6 shows densification curves at varying MgO levels for silicon nitride hot-pressed at constant temperature and pressure. Instantaneous densification rates at a density of 0.70 derived from Fig. 6 are then plotted against MgO content as shown in Fig. 7. Good linearity is observed over the range of concentrations where MgO is present as a silicate phase; the presence of free excess MgO, which can be detected as periclase by X-ray diffraction in specimens containing more than 15 wt% MgO, results in a lowering of the densification rate.

The linearity of Fig. 7 is not expected on the basis of either diffusional creep or viscous flow mechanisms. Since a second phase is present, the activity of MgO is expected to be relatively constant at the Si_3N_4/second phase interface; consequently, arguments based on the ability of MgO in solid solution to control the concentration of the rate controlling defect in the Si_3N_4 grains would not explain the linearity. Viscous flow mechanisms are expected [18] to depend upon W^3 and may therefore be also excluded on the basis of the linear observations. The conclusion is, in sum, that densification is controlled by diffusion of material through the second phase in the grain boundary.

If it is assumed that the liquid phase is of eutectic composition the amount of liquid for a given MgO level can be calculated and hence, knowing the surface area of the powder, an estimate for W can be obtained. All the geometric terms in Equation 3 are now known and the process diffusion coefficient (D_b) can be calculated. This has been done for silicon nitride containing 5 wt% MgO hot-pressed at 21 MN m^{-2} and the results are shown in the Arrhenius plot, Fig. 8.

The calculation is made on the basis of control by silicon ion diffusion in the grain-boundary phase; under these conditions, a^3 is given by $\frac{1}{3}$ of the molecular volume, V, of silicon nitride. Control by nitrogen ion diffusion ($a^3 = \frac{1}{4}V$) would raise the D_b values by 25%. The plot shows clearly the existence of two regions, the migration enthalpies for diffusion in the boundary being 450 kJ mol^{-1} and 695 kJ mol^{-1} above and below 1550° C respectively. Since the eutectic in the $MgSiO_3$–SiO_2 system occurs at 1543° C, the simplest explanation for the two energies is that they represent diffusion in a second phase boundary region which does or does not contain a liquid phase as one of its elements. The specific values for the boundary diffusion coefficient D_b are

$$D_b = 10^{-1.9}\exp\frac{-450\,000}{(RT)}$$

above 1550° C, and

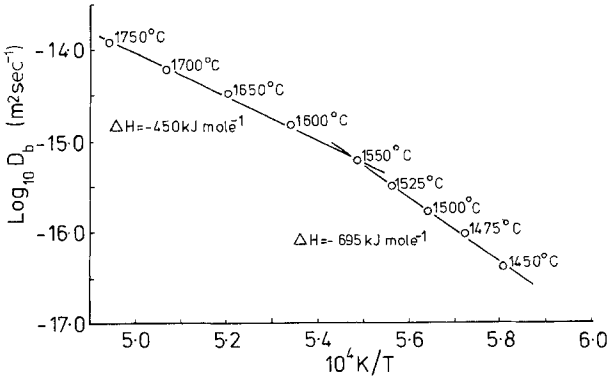

Figure 8 Arrhenius plot of process diffusion coefficient, D_b, for silicon nitride containing 5% MgO pressed at 20 MN m^{-2}.

$$D_b = 10^{4.2} \exp \frac{-695\,000}{(RT)}$$

below this temperature.

3.4. Phase transformation kinetics

In the absence of additives, no α to β silicon nitride conversion was detected at temperatures up to 1750° C, even after very prolonged periods of hot-pressing. However, conversion occurred in compacts containing a few percent of magnesia at temperatures over 1400° C and was complete in only 30 min at 1750° C. These findings agree with those of Messier and Riley [19] for highly pure CVD α silicon nitride, although in the latter instance it was found possible to observe conversion without additives at 1600° C in less pure AME material.

The time dependence of the conversion is shown in Fig. 9 for compacts containing 5% MgO hot-pressed under 20 MN m^{-2} pressure at various temperatures in the range 1550 to 1750° C. Each point on the curves represents an individual hot-pressing held for the specified time at temperature. For temperatures over 1650° C the conversion is so rapid that the time taken to reach the required temperature is significant in comparison with the hold-time at temperature; hence the curves do not extrapolate back to the same initial α content. Comparison of the data in Fig. 9 with data for densification of the same silicon nitride powder (Fig. 2) shows that approximately 12% conversion occurs during densification.

The data of Fig. 9 suggest that the conversion kinetics are first order, as defined by the equation:

$$\frac{d\alpha}{dt} = -K\alpha \qquad (4)$$

where K = rate constant, and α is the concentration of the α phase in the sample. The linear fit of the data to a log α versus time plot (Fig. 10) supports this interpretation. Fig. 11 shows the temperature dependence of the conversion in the form of an Arrhenius plot constructed using the K values obtained from Equation 4 over the temperature

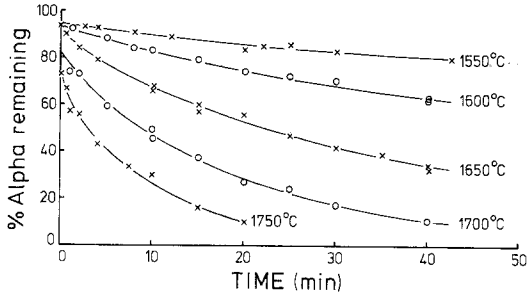

Figure 9 Time dependence of conversion of α to β silicon nitride containing 5% MgO. Each point represents an individual hot-pressing held at the stated temperature, for the specified time.

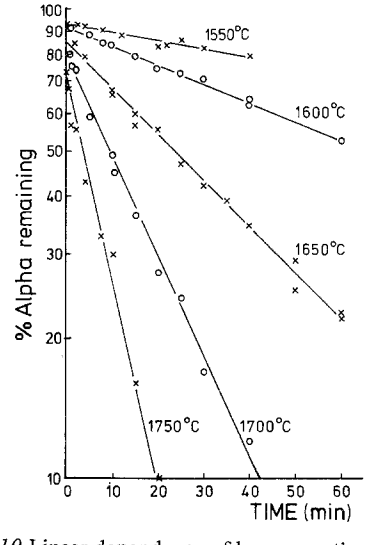

Figure 10 Linear dependence of $\log_{10} \alpha$ on time for silicon nitride containing 5% MgO hot-pressed at 20 MN m^{-2}, indicating first order kinetics.

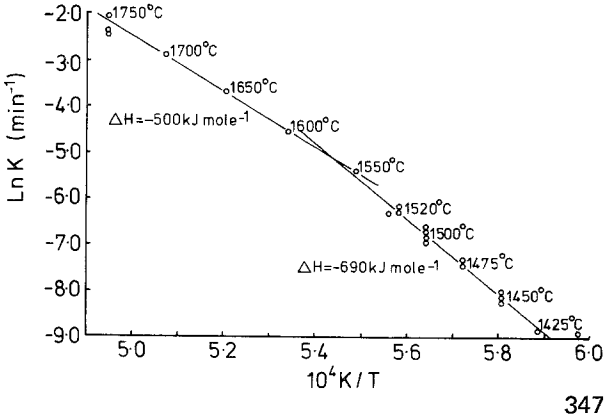

Figure 11 Arrhenius plot of values of K, derived from data in Fig. 10, using Equation 4.

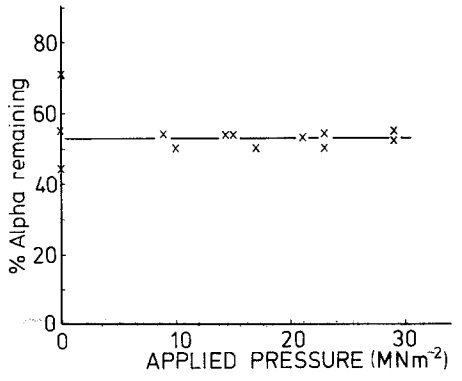

Figure 12 Dependence of degree of conversion under constant hot-pressing conditions (1 h at 1600° C) on applied pressure, for silicon nitride containing 5% MgO.

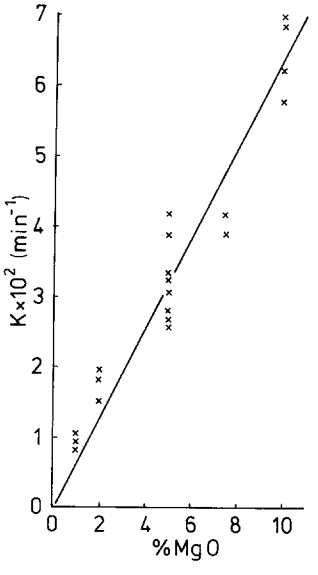

Figure 13 Linear dependence of rate constant, K on MgO content for silicon nitride hot-pressed at 1600° C at a pressure of 21 MN m^{-2}.

range 1400 to 1750° C. The similar temperature dependence of both the conversion and densification data (Fig. 8) is immediately apparent. At approximately 1550° C, a change in activation energy from −690 to −500 kJ mol^{-1} is observed, again correlating with the eutectic temperature in the $MgSiO_3$–SiO_2 system. The activation energies above and below 1550° C are closely similar for both the conversion and densification processes; this suggests that both processes are controlled by diffusion in the boundary phase.

The dependence of the conversion rate on the pressure applied subsequent to densification may be seen in Fig. 12 where percentage conversion after a fixed time is plotted against hot-pressing pressure for theoretically dense compacts; the indication is that the conversion rate is independent of pressure for applied loads up to 30 MN m^{-2}. This is consistent with the fact that enormously greater pressures are generally required to produce significant changes in fully dense solid systems [20].

The geometrical features of the diffusion process responsible for the transformation may be studied by noting the variation of the amount of conversion with additive content under fixed hot-pressing conditions; it is then seen that the conversion rate increases to a maximum at 15% magnesia and then falls. As excess additive becomes detectable as periclase beyond the 15% level, it is reasonable to suggest that the presence of excessive amounts of MgO may retard the conversion. When the conversion data are presented in terms of the dependence of the rate constant K on the MgO added a linear dependence results, as shown in Fig. 13. The increase in rate of conversion with increasing magnesia content indicates that the material transport required for conversion takes place primarily along the grain boundaries rather than across them. In the latter case, a decrease in the additive content would produce a decrease in grain-boundary width, and hence an increase in conversion rate would be expected. Thus, as in the case of the temperature dependence, a similarity is found between the densification rate and the transformation rate in terms of their dependence on the amount of additive.

4. Discussion

The similar dependence of densification (Figs. 7 and 8) and phase transformation (Figs. 13 and 11) on the amount of additive and on temperature points strongly to a similar atomic diffusion mechanism as being responsible for the two processes.

The earlier contention [8] that transformation was not a necessary preliminary to densification remains valid in that complete density can be achieved with some 12% transformation; however, since the elimination of the approximately 30% void space in the initial compact can be achieved by movement of some 15% of the solid material, the relative degree of transformation attained at the point of achievement of full density is consistent with a model in which densification and transformation occur simultaneously as an atom undergoes the solution–diffusion–reprecipitation cycle.

The proposed picture therefore is that atoms,

driven predominantly by the stress gradient imposed by the applied pressure (and hence moving parallel to the boundary), go into solution from the α phase and reprecipitate to the β phase; according to this suggestion, the two phases are seen as polytypes [21] with the β phase the slightly more stable [22] at the temperatures of these experiments.

The similar dependences allow formulation of a combined flux equation [23] for the diffusion process in the early stages of hot-pressing when densification is incomplete. The equation has the form:

$$J = -\frac{AcD}{LRT}(a^3 \Delta P + \Delta G_{tr}), \qquad (5)$$

where A and L are geometrical factors, c the concentration of the diffusing species, ΔP the stress difference between the points of solution and reprecipitation, and ΔG_{tr} the free energy for the α–β transformation. This equation is a convenient means of summarizing the consequences of the proposed model and of identifying any inconsistencies that remain in the suggested interpretation.

The equation is proposed on the ground that the densification rate and the transformation rate are both linearly related to the flux of the rate controlling atoms. The first relation stems from the Coble model [11] and the second stems directly from the proposed picture wherein the diffusing atoms reprecipitate as the β phase.

The argument for linking the two fluxes (for densification and for transformation) in the same equation is based on: (i) the indication that both processes are controlled by an identical diffusion coefficient (Figs. 8 and 11); (ii) the indication that both processes have a similar dependence on the grain boundary geometry (Figs. 7 and 13) so that the A/L term is a common factor.

These results suggest that both densification and transformation are controlled by the same species diffusing in the same direction (parallel to the boundary) in the same medium; consequently the total driving force is seen as the vector sum of the two component energy gradients

$$\frac{a^3 \Delta P + \Delta G_{tr}}{L}.$$

Since the steepest pressure gradient is parallel to the boundaries (from the contact points to the pore/boundary interface) and the steepest chemical free energy gradient is that across the shortest distance between α and β grains (normal to the boundary between the two), the combined equation suggests that $a^3 \Delta P > \Delta G_{tr}$ in order that the parallel movement predominates. Using the experimental values for the applied pressure, the value of $a^3 \Delta P$ is typically $1000\,\mathrm{J\,mol^{-1}}$ which would imply a small value for ΔG_{tr} but one not inconsistent with the polytype form of phase change [24].

As a consequence of Equation 5 one would expect: (i) a linear dependence of both densification rate and transformation rate on the applied pressure during the early stages of processing before the achievement of full density. The first was observed (Fig. 3); the second could not be explored owing to the short time span between the application of pressure and the achievement of full density, and the small amount of transformation attained in that interval.

As another result of the model, it is predicted that: (ii) a pressure-independent transformation rate should be observed following densification. This is indeed found as shown in Fig. 12.

Comparison between (i) and (ii) shows that the transformation rate should change at the point at which full densification is achieved. Further, the dependence of the rate on the additive content should also change at this point. As noted earlier, although transformation data in the MgO-doped Si_3N_4 system are difficult to record in the short time span before full density is achieved (compare Figs. 2 and 9), evidence for such changes in rate is not afforded by the data obtained in this study (Figs. 9 and 10).

In summary, it is believed that the combined Equation 5 and the proposed model are in good agreement with results taken prior to complete densification. The applicability of the model following densification (when $a^3 \Delta P = 0$) is more open to question, the unresolved features being the absence of a break in the transformation curves at the point of full density and the continued linear dependence on additive content in the fully dense state. Although the latter can perhaps be explained by futher growth of β grains seeded during the densification stage, there would be value in studying a system where the relative rate of densification to that of transformation were less pronounced. In this last respect, it appears that a study of the Y_2O_3/Si_3N_4 system may well be helpful.

5. Conclusions

Two mechanisms of densification of α silicon nitride when using MgO as an additive have been identified. The first is a very rapid particle rearrangement stage, which is liquid-enhanced above 1550° C, and which operates up to relative densities of about 0.65. A small contribution to this stage may be made by particle deformation above 1450° C.

The second much slower and decelerating stage involves particle reshaping by diffusion of Si/N through a magnesium silicate grain boundary phase away from regions of high stress between particles. The rate of deformation under otherwise comparable conditions is proportional to the amount of this grain boundary phase and hence to the concentration of MgO additive. Similar diffusion through a solid grain boundary phase is probably responsible for the slow densification observable below 1550° C.

The α to β phase transformation follows first order kinetics. It shows striking similarity to the densification process in terms of the linear dependence of the observed rate on the amount of additive and in terms of the form of the dependence of the rate on temperature.

It is proposed that both processes are controlled by the solution–diffusion–reprecipitation of either Si or N, with the diffusion step being rate-controlling. The diffusion coefficient in the boundary phase is

$$D_b = 10^{-1.9} \exp \frac{-450\,000}{(RT)}$$

above 1550° C and

$$D_b = 10^{4.2} \exp \frac{-695\,000}{(RT)}$$

below this temperature.

Acknowledgements

The authors wish to acknowledge the provision by the Science Research Council of a Research Grant and two Research Studentships (for RJW and LJB) which enabled this work to be carried out.

References

1. A. ATKINSON, A. J. MOULSON and E. W. ROBERTS, *J. Amer. Ceram. Soc* **59** (1976), 285.
2. P. DREW and M. H. LEWIS, *J. Mater. Sci.* **9** (1974), 261.
3. B. D. POWELL and P. DREW, *ibid.* **9** (1974), 1867.
4. S. HOFMANN and L. J. GAUCKLER, *Powder Met. Int.* **6** (1974), 90.
5. G. R. TERWILLIGER and F. F. LANGE, *J. Amer. Ceram. Soc.* **57** (1974), 25.
6. D. HARDIE and K. H. JACK, *Nature* **180** (1957), 332.
7. British Patent 1,092,637 (1964).
8. R. J. WESTON and T. G. CARRUTHERS, *Proc. Brit. Ceram. Soc.* **22** (1973), 197.
9. S. WILD, P. GRIEVESON and K. H. JACK, *Special Ceramics* **5** (P. Popper, ed.) (1972), 377.
10. F. R. N. NABARRO, "The Strength of Solids", (London Physical Society, London, 1948) p. 75. C. HERRING, *J. App. Phys.* **21** (1950) 437.
11. R. L. COBLE, *J. App. Phys.* **34** (1963), 1679.
12. W. D. KINGERY, *ibid* **30** (1959), 301.
13. J. WEERTMAN, *ibid* **28** (1957), 1185.
14. R. C. ROSSI and R. M. FULRATH, *J. Amer. Ceram. Soc.* **48** (1965), 558.
15. P. MURRAY, D. T. LIVEY and J. WILLIAMS, "Ceramic Fabrication Processes" edited by W. D. Kingery (Wiley, New York, 1958) 147.
16. R. L. COBLE, *J. App. Phys.* **41** (1970), 4798.
17. L. J. BOWEN, R. J. WESTON, T. G. CARRUTHERS and R. J. BROOK, *Ceramurgia International* **2** (1976), 173.
18. F. F. LANGE, "Deformation of Ceramic Materials" edited by R. C. Bradt and R. E. Tressler (Plenum Press, New York, 1975) p. 361.
19. D. MESSIER and F. L. RILEY, Paper presented at the NATO ASI 'Nitrogen Ceramics', Canterbury, 1976.
20. R. S. BRADLEY and D. C. MUNRO, "High Pressure Chemistry" (Pergamon, Oxford, 1965).
21. D. S. THOMPSON and P. L. PRATT, *Science of Ceramics* **3** (1967), 33.
22. C. M. B. HENDERSON and D. TAYLOR, *Trans. Brit. Ceram. Soc.* **74** (1975), 49.
23. R. J. BROOK, T. G. CARRUTHERS, L. J. BOWEN and R. J. WESTON, paper presented at the NATO ASI 'Nitrogen Ceramics', Canterbury, 1976.
24. A. R. VERMA and P. KRISHNA. "Polymorphism and Polytypism in Crystals" (Wiley, New York, 1966).

Received 27 April and accepted 20 May 1977.